A&A 366, 662–667 (2001)
DOI: 10.1051/0004-6361:20000244

Astronomy & Astrophysics

Polyatomic species in diffuse cloud and clump interfaces

T. K. Nguyen[1], T. W. Hartquist[2], and D. A. Williams[1]

[1] Department of Physics and Astronomy, University College London, Gower Street, London, WC1E 6BT, UK
[2] Department of Physics and Astronomy, University of Leeds, Leeds LS2 9JT, UK

Received 6 June 2000 / Accepted 13 November 2000

Abstract. Diffuse clouds embedded in a flowing intercloud medium will develop warm interface layers in which the thermal pressures should significantly exceed those within the cloud. We have investigated the gas-phase formation of polyatomic molecules within such warm interfaces. If an interface occupies a few percent of the total molecular column density along that line-of-sight, then many polyatomic species in that interface should have detectable abundances. We have compared the results of interface models with observational data on polyatomic species obtained by Liszt and Lucas. Some models give results that are in harmony with measured ratios of several species including C_2H, HCO^+ and OH; these models have background radiation fields intensities that are lower than the standard by an order of magnitude. The number densities of molecular hydrogen are of the order of 10^2 cm^{-3} in regions with temperatures of several thousand degrees. Such conditions in an interface do not conflict with the lower pressures inferred from CO data, as most of the CO is expected to be in the cold bulk of the material rather than in interfaces. The constancy of the sum of MHD wave "pressure" and thermal pressure implies higher thermal pressures in interfaces than in the cold cloud and cold clump material. The radiation and thermal pressure conditions required to explain the observed abundance ratios may be more likely in interfaces around diffuse clumps within Giant Molecular Clouds than those around the isolated "field" diffuse clouds observed in ultraviolet absorption. Some measured abundance ratios, the most notable of which is that of the abundances of H_2CO and HCO^+, are not well matched by model results, though on the basis of the models the relevant species would be expected to be observable in some cases. It is possible that the adopted chemical network is incomplete.

Key words. ISM: abundances; clouds; molecules

1. Introduction

Lucas & Liszt (1993, 1996, 2000a,b) and Liszt & Lucas (1995, 1998, 2000) have observed a number of diatomic and polyatomic species in millimetre wavelength absorption against background extragalactic sources along lines-of-sight through diffuse interstellar clouds. Liszt & Lucas (1999) recently presented a short summary of the results, while Lucas & Liszt (1997) gave a more detailed, earlier review of their work. The low column densities of CO (in the range of 10^{14} cm^{-2} to 10^{16} cm^{-2}) and its fractionation constrain most of it to be in cold diffuse material where much of the carbon is in the form of C^+. In addition to CO, the species detected in absorption include HCO^+, OH, CN, HCN, HNC, C_2H, H_2CO, C_3H_2, CS, SO, H_2S and SiO. Liszt & Lucas (1999) noted that the presence of many of these species in the detected abundances is a mystery similar to that of the high abundances measured for CH^+ in diffuse clouds.

A number of explanations, summarized by van Dishoeck (1998), have been offered as solutions to the CH^+ problem. (Indeed, a complete review of them would touch on a good fraction of the history of the field of interstellar chemistry). Some work on the origins of the diffuse cloud polyatomics follows ideas already applied in the CH^+ problem. Line profile data (e.g. Liszt & Lucas 2000) present difficulty for shock models (Flower & Pineau des Forêts 1998), and it is probable that (if they operate) the speculative nonlinear effects invoked by Joulain et al. (1998) lead to dissipation through shock formation and are similarly constrained. One of the explanations examined by Duley et al. (1992) concerns the possibility that CH^+ is abundant in the interface regions between cold clumps and more tenuous, hotter media flowing around them. Here we investigate the possibility that the polyatomic species detected by Liszt and Lucas are formed in such interface regions.

Section 2 describes briefly the physical properties likely to be obtained in the interfaces. Section 3 contains a summary of the assumptions made in the construction of the

Send offprint requests to: T. K. Nguyen,
e-mail: tkn@star.ucl.ac.uk

Article published by EDP Sciences and available at http://www.aanda.org or http://dx.doi.org/10.1051/0004-6361:20000244

chemical models and calculated fractional abundances for the models. Section 4 presents a discussion of our results, and we make a short conclusion in Sect. 5.

2. Turbulent boundary layers

The tenuous intercloud medium surrounding a diffuse cloud almost certainly flows around the cloud since stellar winds and supernovae drive flows throughout the intercloud medium. The flow may be of fairly moderate to low Mach number (M), in which case the cloud can be confined for a time substantially in excess of its fast-mode magnetosonic crossing time. However, even if the tenuous material flows at a fairly low Mach number relative to a cloud, the flow establishes pressure differences on the cloud surface as a consequence of the Bernoulli effect. Cloud material will move to the region of the surface where the pressure is lowest at a speed of order $M^2 c_{\rm f}$, where $c_{\rm f}$ is the fast-mode speed in the cloud (e.g. Hartquist & Dyson 1988) for all but very small values of M. Thus, H_2 will reach the surface of a diffuse cloud (Hartquist et al. 1992). There it is heated due to the dissipation of waves generated by the Kelvin-Helmholtz instability occurring at the cloud-intercloud interface. As discussed by Duley et al. (1992) the heating may result in temperatures of many hundreds or even thousands of degrees in H_2-rich gas moving at speeds well below $c_{\rm f}$ with respect to the bulk of the cloud. The scenario is depicted in Fig. 1.

Duley et al. (1992) assumed that the gas in the interface would be at a thermal pressure comparable to the thermal pressure of the cloud. In fact, if the motions giving rise to the broadening of spectral features in the cloud are very superthermal, the thermal pressure in some parts of the interface region may well substantially exceed the thermal pressure in the cloud. In the vicinity of a steady interface structure the sum of the wave and thermal pressures must be nearly constant along a largescale magnetic field line; within the WKB approximation (e.g. Barnes 1992) the wave pressure goes up as $\rho^{1/2}$, where ρ is the density. If the superthermal motions in clouds are due to waves generated at their surfaces propagating into them (e.g. Coker et al. 2000) the thermal pressure in the low density part of the interface regions will exceed the thermal pressure in the bulk of the cloud.

The fraction, f, of the total pressure acting along a large-scale magnetic field line, $P_{\rm tot}$, that is thermal pressure, $P_{\rm th}$, can be calculated from:

$$f \equiv \frac{P_{\rm th}}{P_{\rm tot}} \tag{1}$$

$$P_{\rm th} = \frac{k_{\rm B}\,\rho\,T}{\mu} \tag{2}$$

$$P_{\rm tot} = P_{\rm th} + U \tag{3}$$

where $k_{\rm B}$ is Boltzmann's constant, ρ is the density, T is the temperature, μ is the mean mass per particle, and U is the time-averaged energy density of the perturbation

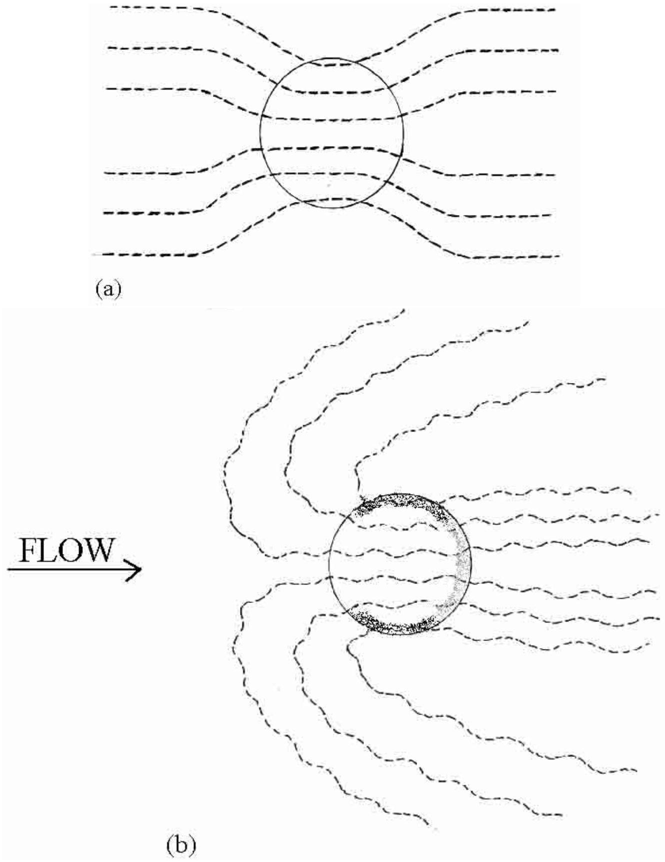

Fig. 1. The Magnetic Field and Thermal Structures of a Diffuse Cloud. **a)** The intercloud medium is static. The magnetic field lines are somewhat bent as the field contributes to the support of the cloud against the pressure of the intercloud medium. **b)** A subsonic flow engulfs the cloud. Magnetic field lines are bent around the cloud by the flow. The existence of hydromagnetic waves is indicated by undulations in the field lines and is likely to be a consequence of the flowing intercloud medium with the cloud. The shaded regions are those to which H_2 flows most rapidly to the surface; the shading is darkest in those interface regions containing H_2 where the viscous heating rate is probably greatest

magnetic field (e.g. Martin et al. 1997). If the wave is an Alfvén wave and V is its velocity amplitude, and subscript "c" indicates that the quantity is equivalent at the cold side of the interface,

$$U = \frac{1}{4}\,\rho_{\rm c}\,V_{\rm c}^2\,\left(\frac{\rho}{\rho_{\rm c}}\right)^{1/2}. \tag{4}$$

Equation (4) is correct in the WKB-limit. It follows that,

$$\frac{f}{f_{\rm c}} = \frac{1}{f_{\rm c}} - \frac{(1-f_{\rm c})}{f_{\rm c}}\,\left(\frac{\rho}{\rho_{\rm c}}\right)^{1/2} \tag{5}$$

and

$$\left(\frac{\rho}{\rho_{\rm c}}\right)^{1/2} = -\frac{(1-f_{\rm c})}{2f_{\rm c}}\,\frac{T_{\rm c}}{T} + \left[\frac{(1-f_{\rm c})^2}{4f_{\rm c}^2}\,\frac{T_{\rm c}^2}{T^2} + \frac{T_{\rm c}}{f_{\rm c}T}\right]^{1/2}. \tag{6}$$

Table 1. The elemental abundances relative to that of hydrogen nuclei

Species	Elemental Abundance
H	$0.0\ 10^{-00}$
He	$7.1\ 10^{-02}$
C	$3.0\ 10^{-04}$
N	$2.0\ 10^{-05}$
O	$6.0\ 10^{-02}$
S	$3.0\ 10^{-06}$
Mg	$3.0\ 10^{-09}$
Na	$1.0\ 10^{-06}$
Si	$1.0\ 10^{-06}$

For $V_c = 3$ km s^{-1} and $T_c = 100$ K, then $f_c \simeq 0.13$, implying that the thermal pressure in warm regions of the interface is about 7 times that in the cooler regions.

Duley et al. (1992) limited their considerations to interface gas with thermal pressure comparable to the highest thermal pressures thought to be associated with diffuse molecular clouds observed with Copernicus. However, observations of those clouds showed evidence of superthermal motions. Consequently, we will consider here interface region pressures substantially exceeding the thermal pressures of the diffuse molecular clouds, as well as more modest interface region pressures.

3. The chemical model

We argued in the previous section that H_2-rich gas will move to the vicinity of a cloud surface where the pressure is lowest rapidly enough that little of the H_2 in it will be photodissociated. Therefore, we assume that all hydrogen entering the interface is initially H_2 and that its photodissociation rate is negligible. All elements whose neutral atoms have ionization potentials less than that of hydrogen were assumed to be in the form of singly charged atomic ions (e.g. C^+ and S^+, etc.) initially, while all other elements were taken to be in neutral atomic form. The number density of hydrogen nuclei, n_H, and T, were held constant. Integrations of the chemical rate equations were halted after about 10^4 years, by which time the abundances of all species of interest had reached steady-state. The assumed elemental abundances relative to that of hydrogen are given in Table 1. The UMIST chemical database (Millar et al. 1997) was used, and the model followed the time-dependence of 337 species interacting in 2950 chemical reactions.

Table 2 displays the model results for the fractional abundances of selected species relative to n_H for a range of values of the parameters n_H, $n_H T$ and also χ, a measure of the incident radiation field which is unity for the standard interstellar background radiation field.

4. Discussion

Warm interface regions are likely to contain only a few percent of the column density of a cloud. Therefore for a species Y to have a column density of about 10^{12} cm^{-2} in a warm interface of a diffuse cloud it must have a fractional abundance, $X(Y)$, relative to n_H of about $3\ 10^{-8}$. A number of the models listed in Table 2 give fractional abundances of this magnitude and greater for a variety of the species observed in millimetre wave absorption. However only a few models give abundance ratios of key polyatomic species similar to those measured.

We focus first on the C_2H to HCO^+ abundance ratio which Lucas & Liszt (2000b) have found to vary but often to have a value in the range 10 to 20. Models 11 and 18 are the only ones with values of that ratio in that range, while the values for models 12 and 17 are greater. Of these four models, only model 11 has an OH to HCO^+ abundance ratio within rough agreement with the measured values which almost uniformly are between about 20 to 30 (Lucas & Liszt 1996). For models 12 and 17, as well as for models 11 and 18, $\chi = 0.1$. That χ must be somewhat lower than usually assumed is probably not a serious constraint. As the observations are made over long line-of-sight, the locations of many of the absorbing diffuse clouds are most likely uncertain. In fact, the use of such background sources may well introduce selection effects favouring the detection of clouds in regions with low values of χ. Clouds in regions with large values of χ may well contain less than the lowest detectable column density of CO. It is likely that a number of the diffuse clumps may reside in or around Giant Molecular Clouds and that the material in such complexes at least partially shields the detected diffuse clouds from the general interstellar radiation field.

The values of $n_H T$ for the models having C_2H to HCO^+ and OH to HCO^+ abundance ratios in rough agreement with the measured ratios are one to one and a half orders of magnitude higher than the value of $n_H T$ that Duley et al. (1992) suggested is compatible with a warm interface being the site of CH^+ and a component of CH observed by Lambert et al. (1990) towards the ζ Oph cloud. However, as CH^+ data do not exist for the lines-of-sight studied by Liszt & Lucas, considerations of its production should not be used as too stringent a constraint in the discussion of the models for the polyatomic data. Optical and ultraviolet absorption studies, like those in which CH^+ is detected, are normally aimed at the investigation of somewhat isolated or "field" diffuse clouds. As mentioned above, along the line-of-sight to an extragalactic source a fair fraction of the diffuse structures (for which the total visual extinction optical depths are unity or less) intercepted may be clumps associated with Giant Molecular Clouds (GMCs). Many of these GMCs have MHD wave "pressures" (e.g. Williams et al. 1995) comparable to the thermal pressures required for the interface models to have abundance ratios of C_2H, HCO^+ and OH similar to those measured by Lucas & Liszt (1996, 2000b).

Table 2. Results from Models 1–54 at time 1 10^4 years. Notation 1.80(−09) ≡ 1.80 10^{-09}

Model	T (K)	nT (cm^{-3} K)	χ	X(CH)	X(CH$^+$)	X(CN)	X(OH)	X(H$_2$O)	X(CO)	X(NH)	X(C$_2$)	X(HCO$^+$)	X(H$_2$CO)	X(HCN)	X(HNC)	X(C$_2$H)	X(C$_3$H$_2$)	X(CS)
1	7(02)	4(03)	0.1	9.92(−07)	6.95(−08)	1.20(−10)	1.69(−06)	4.37(−08)	2.07(−08)	–	2.28(−08)	4.26(−08)	–	2.55(−11)	2.88(−11)	1.17(−08)	–	9.37(−11)
2	7(02)	1(04)	0.1	2.41(−06)	5.91(−08)	6.33(−10)	3.93(−06)	2.23(−07)	1.22(−07)	–	1.91(−07)	9.21(−08)	5.03(−11)	2.36(−10)	8.33(−11)	9.60(−08)	2.16(−11)	6.36(−10)
3	7(02)	4(04)	0.1	6.12(−06)	4.02(−08)	1.02(−08)	1.15(−05)	1.94(−06)	1.66(−06)	–	2.86(−06)	3.18(−07)	2.06(−09)	6.64(−09)	3.68(−10)	1.39(−06)	1.18(−09)	1.06(−08)
4	7(02)	1(05)	0.1	6.73(−06)	2.37(−08)	3.59(−08)	1.91(−05)	6.37(−06)	5.96(−06)	1.03(−11)	6.25(−06)	6.70(−07)	9.25(−09)	3.45(−08)	6.55(−10)	3.10(−06)	6.01(−09)	4.07(−08)
5	7(02)	4(05)	0.1	3.25(−06)	7.26(−09)	8.23(−08)	2.94(−05)	3.27(−05)	2.35(−05)	1.14(−11)	4.36(−06)	1.90(−06)	2.38(−08)	2.18(−07)	1.98(−09)	2.89(−06)	1.80(−08)	8.53(−08)
6	7(02)	1(06)	0.1	1.07(−06)	2.47(−09)	1.31(−07)	3.51(−05)	1.28(−04)	4.15(−05)	1.10(−11)	2.14(−06)	2.76(−06)	2.24(−08)	9.83(−07)	1.82(−08)	1.97(−06)	2.35(−08)	7.65(−08)
7	2(03)	4(03)	0.1	1.22(−05)	6.41(−06)	2.92(−09)	1.32(−04)	2.98(−05)	4.68(−07)	1.14(−07)	2.73(−07)	9.17(−06)	1.62(−09)	3.30(−09)	9.32(−10)	1.54(−07)	1.24(−10)	3.66(−10)
8	2(03)	1(04)	0.1	2.06(−05)	3.15(−06)	9.74(−09)	2.00(−04)	1.10(−04)	1.61(−06)	2.70(−07)	1.37(−06)	1.39(−05)	1.28(−08)	2.57(−08)	2.55(−09)	8.22(−07)	2.06(−09)	2.37(−09)
9	2(03)	4(04)	0.1	2.42(−05)	6.98(−07)	5.69(−08)	1.65(−04)	3.52(−04)	3.58(−06)	8.25(−07)	6.29(−06)	9.21(−06)	6.21(−08)	5.47(−07)	8.66(−09)	4.15(−06)	2.87(−08)	1.69(−08)
10	2(03)	1(05)	0.1	2.06(−05)	2.03(−07)	1.09(−07)	9.21(−05)	4.79(−04)	3.38(−06)	1.22(−06)	1.03(−05)	3.98(−06)	6.62(−08)	2.49(−06)	1.61(−08)	7.19(−06)	7.84(−08)	4.35(−08)
11	2(03)	4(05)	0.1	1.13(−05)	2.30(−08)	7.81(−08)	3.00(−05)	5.63(−04)	1.84(−06)	7.78(−07)	1.31(−05)	6.37(−07)	2.73(−08)	6.56(−06)	2.60(−08)	9.90(−06)	1.90(−07)	1.12(−07)
12	2(03)	1(06)	0.1	6.62(−06)	4.86(−09)	4.09(−08)	1.49(−05)	5.82(−04)	1.13(−06)	3.28(−07)	1.37(−05)	1.59(−07)	1.13(−08)	7.64(−06)	3.47(−08)	1.07(−05)	2.78(−07)	1.66(−07)
13	4(03)	4(03)	0.1	1.18(−05)	2.21(−05)	8.70(−09)	2.88(−04)	1.46(−04)	4.06(−07)	3.86(−06)	1.51(−07)	1.87(−05)	7.15(−09)	5.14(−08)	1.75(−09)	8.74(−08)	4.36(−11)	1.61(−10)
14	4(03)	1(04)	0.1	2.53(−05)	1.08(−05)	2.60(−08)	2.37(−04)	2.83(−04)	9.84(−07)	6.49(−06)	8.71(−07)	1.79(−05)	2.22(−08)	3.65(−07)	5.07(−09)	5.50(−07)	1.26(−09)	1.65(−09)
15	4(03)	4(04)	0.1	2.83(−05)	2.08(−06)	4.61(−08)	1.22(−04)	4.56(−04)	1.03(−06)	7.20(−06)	4.03(−06)	4.22(−06)	3.71(−08)	2.30(−06)	1.21(−08)	3.02(−06)	2.06(−08)	1.36(−08)
16	4(03)	1(05)	0.1	1.91(−05)	4.98(−07)	3.69(−08)	7.81(−05)	5.11(−04)	7.90(−07)	5.36(−06)	7.15(−06)	1.15(−06)	2.67(−08)	3.86(−06)	1.38(−08)	5.74(−06)	5.95(−08)	2.58(−08)
17	4(03)	4(05)	0.1	1.37(−05)	6.29(−08)	2.99(−08)	7.13(−05)	5.19(−04)	9.54(−07)	4.05(−06)	1.46(−05)	2.35(−07)	1.41(−08)	5.39(−06)	2.14(−08)	1.36(−05)	2.07(−07)	4.37(−08)
18	4(03)	1(06)	0.1	4.33(−05)	8.49(−08)	9.59(−08)	1.59(−04)	3.88(−04)	8.13(−06)	3.32(−06)	1.05(−05)	8.06(−07)	1.44(−08)	7.10(−06)	5.09(−08)	1.52(−05)	3.57(−07)	9.69(−08)
19	7(02)	4(03)	0.3	2.91(−07)	9.32(−08)	2.60(−11)	5.82(−07)	5.90(−09)	9.39(−09)	–	1.86(−09)	2.06(−08)	–	–	–	9.61(−10)	–	–
20	7(02)	1(04)	0.3	8.18(−07)	7.21(−08)	8.95(−11)	1.42(−06)	3.08(−08)	4.44(−08)	–	1.52(−08)	3.69(−08)	–	1.72(−11)	2.33(−11)	7.80(−09)	–	6.37(−11)
21	7(02)	4(04)	0.3	3.01(−06)	5.52(−08)	1.07(−09)	5.02(−06)	3.59(−07)	6.27(−07)	–	3.35(−07)	1.18(−07)	1.05(−10)	4.51(−10)	1.11(−10)	1.67(−07)	4.89(−11)	1.12(−09)
22	7(02)	1(05)	0.3	5.26(−06)	4.22(−08)	5.53(−09)	1.00(−05)	1.45(−06)	3.23(−06)	–	1.60(−06)	2.60(−07)	9.21(−10)	3.18(−09)	2.48(−10)	7.74(−07)	5.26(−10)	6.31(−09)
23	7(02)	4(05)	0.3	5.11(−06)	1.99(−08)	2.37(−08)	2.00(−05)	7.66(−06)	2.04(−05)	–	3.35(−06)	7.34(−07)	4.40(−09)	2.41(−08)	4.61(−10)	1.59(−06)	3.41(−09)	3.26(−08)
24	7(02)	1(06)	0.3	2.49(−06)	8.61(−09)	3.30(−08)	2.62(−05)	2.28(−05)	5.03(−05)	–	1.98(−06)	1.48(−06)	5.85(−09)	6.85(−08)	9.20(−10)	1.12(−06)	5.57(−09)	4.11(−08)
25	2(03)	4(03)	0.3	3.00(−06)	1.03(−05)	7.01(−10)	5.56(−05)	4.23(−06)	2.40(−07)	3.84(−08)	1.89(−08)	4.59(−06)	6.52(−11)	3.36(−10)	1.97(−10)	1.01(−08)	–	2.90(−11)
26	2(03)	1(04)	0.3	9.67(−06)	6.81(−06)	2.15(−09)	1.14(−04)	2.10(−05)	1.10(−06)	9.24(−08)	1.68(−07)	8.59(−06)	8.66(−10)	2.03(−09)	6.79(−10)	9.31(−08)	7.27(−11)	3.22(−10)
27	2(03)	4(04)	0.3	2.14(−05)	2.26(−06)	1.13(−08)	2.03(−04)	1.39(−04)	6.61(−06)	3.08(−07)	1.56(−06)	1.52(−05)	1.32(−08)	3.63(−08)	2.75(−09)	9.15(−07)	2.54(−09)	3.54(−09)
28	2(03)	1(05)	0.3	2.40(−05)	8.77(−07)	3.38(−08)	1.78(−04)	2.87(−04)	1.33(−05)	5.57(−07)	3.78(−06)	1.45(−05)	2.62(−08)	2.50(−07)	5.58(−09)	2.27(−06)	1.13(−08)	1.13(−08)
29	2(03)	4(05)	0.3	2.02(−05)	1.71(−07)	1.08(−07)	8.15(−05)	4.68(−04)	1.88(−05)	6.21(−07)	8.82(−06)	6.55(−06)	2.19(−08)	2.85(−06)	1.63(−08)	5.47(−06)	5.55(−08)	4.41(−08)
30	2(03)	1(06)	0.3	1.59(−05)	5.11(−08)	7.28(−08)	4.31(−05)	5.27(−04)	1.72(−05)	2.04(−07)	1.20(−05)	2.63(−06)	1.31(−08)	4.27(−06)	2.00(−08)	7.73(−06)	1.14(−07)	8.17(−08)
31	4(03)	4(03)	0.3	1.65(−06)	2.75(−05)	1.56(−09)	2.23(−04)	3.78(−05)	2.57(−07)	1.53(−06)	7.89(−09)	1.53(−05)	4.68(−10)	3.26(−09)	3.05(−10)	4.23(−09)	–	–
32	4(03)	1(04)	0.3	8.19(−06)	2.23(−05)	6.20(−09)	2.77(−04)	1.09(−04)	1.24(−06)	3.18(−06)	9.74(−08)	2.66(−05)	3.95(−09)	2.92(−08)	1.22(−09)	5.38(−08)	4.47(−11)	1.85(−10)
33	4(03)	4(04)	0.3	2.93(−05)	8.36(−06)	3.71(−08)	2.29(−04)	2.78(−04)	3.90(−06)	6.37(−06)	1.12(−06)	1.96(−05)	1.91(−08)	5.91(−07)	6.12(−09)	6.89(−07)	2.56(−09)	3.50(−09)
34	4(03)	1(05)	0.3	4.04(−05)	3.26(−06)	6.99(−08)	1.78(−04)	3.62(−04)	5.26(−06)	6.39(−06)	2.93(−06)	1.07(−05)	2.41(−08)	2.25(−06)	1.14(−08)	1.97(−06)	1.34(−08)	1.12(−08)
35	4(03)	4(05)	0.3	4.76(−05)	7.41(−07)	8.16(−08)	1.65(−04)	3.76(−04)	9.14(−06)	3.52(−06)	6.31(−06)	4.41(−06)	1.78(−08)	4.50(−06)	1.74(−08)	4.79(−06)	6.46(−08)	3.01(−08)
36	4(03)	1(06)	0.3	4.27(−05)	6.72(−07)	2.01(−07)	2.14(−04)	1.81(−04)	3.09(−05)	1.72(−06)	4.72(−06)	6.82(−06)	4.31(−09)	5.04(−06)	3.04(−08)	4.28(−06)	6.60(−08)	5.61(−08)
37	7(02)	4(03)	1.0	4.82(−08)	1.31(−07)	–	1.77(−07)	8.25(−10)	4.74(−09)	–	8.28(−11)	1.10(−08)	–	–	–	4.29(−11)	–	–
38	7(02)	1(04)	1.0	2.01(−07)	1.02(−07)	1.85(−11)	4.37(−07)	3.38(−09)	1.98(−08)	–	9.32(−10)	1.77(−08)	–	–	–	4.82(−10)	–	–
39	7(02)	4(04)	1.0	9.74(−07)	6.86(−08)	1.17(−10)	1.68(−06)	4.24(−08)	2.04(−07)	–	2.24(−08)	4.20(−08)	–	2.47(−11)	2.81(−11)	1.15(−08)	–	9.21(−11)
40	7(02)	1(05)	1.0	2.25(−06)	5.66(−08)	5.49(−10)	3.89(−06)	2.18(−07)	1.13(−06)	–	1.58(−07)	8.88(−08)	4.04(−11)	1.91(−10)	7.43(−11)	7.95(−08)	1.74(−11)	5.83(−10)
41	7(02)	4(05)	1.0	4.18(−06)	3.55(−08)	3.92(−09)	1.09(−05)	1.75(−06)	1.16(−05)	–	1.00(−06)	2.80(−07)	5.33(−10)	2.08(−09)	1.85(−10)	4.74(−07)	3.45(−10)	5.48(−09)
42	7(02)	1(06)	1.0	3.25(−06)	2.14(−08)	7.86(−09)	1.69(−05)	5.09(−06)	3.91(−05)	–	1.24(−06)	5.42(−07)	1.03(−09)	6.18(−09)	2.75(−10)	5.68(−07)	8.86(−10)	1.23(−08)
43	2(03)	4(03)	1.0	1.91(−07)	8.19(−06)	9.66(−11)	1.82(−05)	4.32(−07)	8.10(−08)	1.16(−08)	2.73(−10)	1.57(−06)	–	2.74(−11)	2.01(−11)	1.45(−10)	–	–
44	2(03)	1(04)	1.0	1.59(−06)	9.93(−06)	4.29(−10)	4.19(−05)	2.34(−06)	4.75(−07)	2.81(−08)	6.71(−09)	3.60(−06)	2.18(−11)	1.72(−10)	1.10(−10)	3.58(−09)	–	1.31(−11)
45	2(03)	4(04)	1.0	9.23(−06)	5.22(−06)	2.12(−09)	1.19(−04)	2.37(−05)	4.39(−06)	9.65(−08)	1.63(−07)	8.37(−06)	8.39(−10)	2.15(−09)	6.43(−10)	8.94(−08)	6.35(−11)	3.61(−10)
46	2(03)	1(05)	1.0	1.47(−05)	2.54(−06)	5.39(−09)	1.74(−04)	7.80(−05)	1.54(−05)	1.88(−07)	6.03(−07)	1.33(−05)	3.61(−09)	1.15(−08)	1.43(−09)	3.33(−07)	4.96(−10)	1.57(−09)
47	2(03)	4(05)	1.0	1.30(−05)	6.59(−07)	1.81(−08)	1.59(−04)	2.32(−04)	5.21(−05)	3.36(−07)	1.81(−06)	1.61(−05)	5.62(−09)	1.23(−07)	3.54(−09)	1.00(−06)	3.19(−09)	6.83(−09)
48	2(03)	1(06)	1.0	9.79(−06)	2.47(−07)	4.27(−08)	1.09(−04)	3.31(−04)	7.54(−05)	3.79(−07)	3.12(−06)	1.15(−05)	3.87(−09)	6.33(−07)	7.38(−09)	1.74(−06)	9.17(−09)	1.57(−08)
49	4(03)	4(03)	1.0	6.10(−08)	1.48(−05)	1.66(−10)	1.03(−04)	5.38(−06)	9.28(−08)	4.93(−07)	7.33(−11)	6.51(−06)	–	1.29(−10)	2.97(−11)	3.90(−11)	–	–
50	4(03)	1(04)	1.0	6.76(−07)	2.27(−05)	8.48(−10)	1.83(−04)	2.19(−05)	7.16(−07)	1.11(−06)	2.25(−09)	1.82(−05)	1.34(−10)	1.31(−09)	1.57(−10)	1.20(−09)	–	–
51	4(03)	4(04)	1.0	6.98(−06)	1.69(−05)	6.51(−09)	2.58(−04)	9.13(−05)	5.00(−06)	2.90(−06)	7.67(−08)	2.74(−05)	2.52(−09)	2.93(−08)	1.16(−09)	4.18(−08)	3.17(−11)	2.41(−10)
52	4(03)	1(05)	1.0	1.63(−05)	9.76(−06)	2.00(−08)	2.48(−04)	1.40(−04)	1.21(−05)	4.09(−06)	3.50(−07)	2.71(−05)	4.99(−09)	1.67(−07)	3.12(−09)	1.95(−07)	3.50(−10)	1.21(−09)
53	4(03)	4(05)	1.0	2.39(−05)	3.85(−06)	7.23(−08)	2.13(−04)	1.17(−04)	3.09(−05)	3.60(−06)	1.14(−06)	2.01(−05)	2.75(−09)	8.97(−07)	7.88(−09)	6.63(−07)	2.35(−09)	6.14(−09)
54	4(03)	1(06)	1.0	8.25(−06)	2.37(−06)	7.29(−08)	1.27(−04)	2.53(−05)	4.07(−05)	1.62(−06)	4.57(−07)	7.95(−06)	1.62(−10)	4.05(−07)	6.09(−09)	2.90(−07)	3.41(−10)	5.68(−09)

We now compare several other measured abundance ratios reviewed by Lucas & Liszt (1997) to those given by the models, with particular emphasis given to model 11. Lucas & Liszt (2000b) give a value of around 30 as the typical measured abundance ratio of C_2H to ortho-C_3H, a value close to that for model 18 but almost a factor of 5 lower than that of model 11. Of course, it should be borne in mind that the reliability of the underlying chemical network becomes more uncertain as the number of atoms, particularly those other than hydrogen, contained in the species under consideration increases. C_3H is in this sense a rather complicated species, and a factor of 5 is not a serious discrepancy. The values for models 11, 12, 17 and 18 of the CN to HCN abundance ratio are all much less than the measured values, as would be expected if CN is a molecule produced in abundance by cold gas phase reactions. Therefore, much of the CN is contained in the cold material. Likewise, interface model CO to HCO^+ abundance ratios are much smaller than measured values, a fact consistent with the great majority of the CO being in cold regions, as demanded by the observations of its extinction. The CS to HCO^+ abundance ratio for model 11 is somewhat lower than typically measured ratios. Better agreement would follow if elemental sulphur were undepleted, as $X(\mathrm{CS})$ scales with the fractional abundance of sulphur (the sulphur abundance in Table 1 implies a depletion by a factor of 5 relative to solar).

The explanation of the millimetre absorption data in terms of the interface models faces some difficulties. Perhaps, the most severe one arises from the data for $X(\mathrm{H_2CO})/X(\mathrm{HCO^+})$. Although H_2CO has not been detected along all lines-of-sight on which HCO^+ is found, it commonly has an abundance ratio that is over one order of magnitude larger than that of model 11 (Liszt & Lucas 1995). However, it should be recalled that no gas-phase chemical model is able to account satisfactorily for diffuse cloud formaldehyde. Consequently, some authors (Viti et al. 1999) have invoked surface reactions on dust. The values of $X(\mathrm{HCN})/X(\mathrm{HCO^+})$ for models giving reasonable values of the ratios $X(\mathrm{C_2H})/X(\mathrm{HCO^+})$ and $X(\mathrm{OH})/X(\mathrm{HCO^+})$ are over one order of magnitude higher than usually measured. Model values of the HNC to HCN abundance ratio are much lower than observed, a fact that may reflect an underlying incompleteness in the treatment of the HNC chemistry rather than a problem with the basic concept behind the models. For example, the reaction network allows the formation of HCN, but not HNC, from the reactants CH_3 and N.

We find that $X(\mathrm{C_2}) \gtrsim 10^{-6}$ for many models. Though it is not detectable in millimetre wave absorption due to its symmetry, C_2 is detectable in absorption in the red against bright enough background stars, and observations of it have been used to constrain temperatures of diffuse molecular clouds to low values (van Dishoeck & Black 1986). Previously measured column densities have been several to many times 10^{13} cm^{-2}. Without more detailed analysis it is difficult to say how stringent the constraints C_2 data place on the properties of warm regions of diffuse clouds towards which it has been observed. χ is most likely greater than 0.3 for most nearby clouds through which C_2 absorption has been detected; that $X(\mathrm{C_2})$ falls with increasing χ in the interface models probably ensures that interface contributions to C_2 features already detected are not dominant.

The high NH abundances in some models are of great interest. The reaction $\mathrm{N} + \mathrm{H_2} \rightarrow \mathrm{NH} + \mathrm{H}$ has a barrier of about 16 000 K (Millar et al. 1997), and NH is not formed efficiently by low temperature gas phase chemistry. Its detection in some lines-of-sight through diffuse clouds has been interpreted as evidence of the importance of grain surface reactions (Wagenblast et al. 1993; Crawford & Williams 1997). Evidently, large amounts of NH may arise in warm interfaces. It is possible that the elevated temperature may promote the surface reaction.

5. Conclusions

Interface regions around a diffuse cloud embedded in a flowing intercloud medium should have thermal pressures that are significantly larger than those within the cloud. In this paper we have explored the gas-phase chemistry arising in such warm interfaces. Our results show that observable abundances of various polyatomic species can be produced if the warm interface regions occupy a few percent of the total molecular column density along that line-of-sight. For models in which the radiation field intensity is about one tenth of the mean interstellar radiation field intensity, then the agreement with observations of Liszt and Lucas is reasonable. However, in some cases the results suggest that the gas-phase chemical network used may be too limited. Surface reactions may also contribute to molecular abundances in both warm interfaces and in the cold cloud gas.

Acknowledgements. We thank an anonymous referee for a very constructive and helpful report which led to a substantial improvement of the discussion.

References

Barnes, A. 1992, JGR, 97, 12105
Coker, R., Rae, J. G. L., & Hartquist, T. W. 2000, A&A, 360, 290
Crawford, I. A., & Williams, D. A. 1997, MNRAS, 291, L53
Duley, W. W., Hartquist, T. W., Sternberg, A., Wagenblast, R., & Williams, D. A. 1992, MNRAS, 255, 463
Flower, D. R., & Pineau des Forêts, G. 1998, MNRAS, 297, 1182
Hartquist, T. W., & Dyson, J. E. 1988, Ap&SS, 144, 615
Hartquist, T. W., Dyson, J. E., & Williams, D. A. 1992, MNRAS, 257, 419
Joulain, K., Falgarone, E., Pineau des Forêts, G., & Flower, D. 1998, A&A, 340, 241
Liszt, H. S., & Lucas, R. 1995, A&A, 299, 847
Liszt, H. S., & Lucas, R. 1998, A&A, 339, 561
Liszt, H. S., & Lucas, R. 1999, BAAS, 194, 4103
Liszt, H. S., & Lucas, R. 2000, A&A, 355, 333
Lucas, R., & Liszt, H. S. 1993, A&A, 276, L33
Lucas, R., & Liszt, H. S. 1996, A&A, 307, 237

Lucas, R., & Liszt, H. S. 1997, in Molecules in Astrophysics: Probes and Processes – IAU Symp. 178, 421, ed. E. F. van Dishoeck (Dordrecht, Kluwer Academic Publishers)
Lucas, R., & Liszt, H. S. 2000a, A&A, 355, 327
Lucas, R., & Liszt, H. S. 2000b, A&A, 358, 1069
Martin, C. E., Heyvaerts, J., & Priest, E. R. 1997, A&A, 326, 1176
Millar, T. J., Farquhar, P. R. A., & Willacy, K. 1997, A&AS, 121, 139
Wagenblast, R., Williams, D. A., Millar, T. J., & Nejad, L. A. M. 1993, MNRAS, 260, 420
Williams, J. P., Blitz, L., & Stark, A. A. 1995, NCSA Astronomy Digital Image Library, 451, 252
van Dishoeck, E. F. 1998, in The Molecular Astrophysics of Stars and Galaxies, 53, ed. T. W. Hartquist & D. A. Williams, Oxford (Oxford Science Publications), 53
van Dishoeck, E. F., & Black, J. H. 1986, ApJ, 307, 332